

Coupled metal–insulator and magnetic transitions in $\text{LnSr}_2\text{Mn}_2\text{O}_7$ (Ln = La, Tb)

Peter D. Battle,* Mark A. Green, N. Scott Laskey, Julie E. Millburn, Matthew J. Rosseinsky,*
Stuart P. Sullivan and Jaap F. Vente

Inorganic Chemistry Laboratory, University of Oxford, South Parks Road, Oxford, UK OX1 3QR

We report magnetisation, conductivity and structural data on the Ruddlesden–Popper $\text{Mn}^{\text{III}}/\text{Mn}^{\text{IV}}$ oxides $\text{LnSr}_2\text{Mn}_2\text{O}_7$ (Ln = La, Tb); while $\text{LaSr}_2\text{Mn}_2\text{O}_7$ undergoes an insulator–metal transition and an increase in spontaneous magnetisation at 132 K, the isostructural terbium compound is semiconducting and paramagnetic throughout the range $4.2 < T/\text{K} < 300$.

The observation of colossal magnetoresistance (strong magnetic field dependence of the electrical resistance) at the Curie temperature (T_c) of $\text{Ln}_{1-x}\text{A}_x\text{MnO}_3$ perovskites (A = Ca, Ba, Sr, Pb) has recently attracted considerable attention.^{1–3} The effect is observed over a narrow range of manganese oxidation states between Mn^{III} ($t_{2g}^3e_g^1$) and Mn^{IV} (t_{2g}^3) in a rich electronic phase diagram—the ground state adopted depends subtly on the band filling and Mn–O–Mn distance and angle, both of which are subject to chemical control. The sharp drop in resistance at T_c shows that spin and charge dynamics are strongly coupled. There is as yet no theoretical consensus for the mechanism producing this effect, but a useful working chemical picture emerges from the Zener–Hasegawa–Anderson double-exchange model wherein ferromagnetic coupling between the localised π^* t_{2g} electrons is mediated by the itinerant e_g σ^* carriers in the metallic state below T_c . In the Ruddlesden–Popper $\text{A}_{n+1}\text{Mn}_n\text{O}_{3n+1}$ series, it is possible to modify the bandwidth of these σ^* electrons by changing the number of Mn nearest-neighbours through the variation of n , the number of connected layers of vertex sharing octahedra. The well known perovskite and K_2NiF_4 structures correspond to $n = \infty$ and $n = 1$, with six and four near-neighbours, respectively. The K_2NiF_4 phases $\text{La}_{1-x}\text{Sr}_{1+x}\text{MnO}_4$ have been shown, in contrast to the perovskites, to become spin-glass insulators rather than ferromagnetic metals on oxidation from Mn^{III} .⁴ $\text{LaSr}_2\text{Mn}_2\text{O}_7$ is an $n = 2$ phase (Fig. 1),^{5,6} the electronic behaviour of which is less well understood than that of the $n = 1$ and $n = \infty$ end members.⁷ Magnetic measurements by previous workers indicate several possible transitions to magnetically ordered ground states. Here we report magnetisation and conductivity measurements on crystallographically and chemically well characterised $\text{LaSr}_2\text{Mn}_2\text{O}_7$ and on the new phase $\text{TbSr}_2\text{Mn}_2\text{O}_7$. We show that $\text{LaSr}_2\text{Mn}_2\text{O}_7$ undergoes a transition to a weak ferromagnetic state at 132 K which, crucially in the search for new colossal magnetoresistance materials, drives an insulator–metal transition.

$\text{LaSr}_2\text{Mn}_2\text{O}_7$ and $\text{TbSr}_2\text{Mn}_2\text{O}_7$ were both prepared by high-temperature solid-state reactions.[†] Rietveld refinement of powder XRD data showed that $\text{LaSr}_2\text{Mn}_2\text{O}_7$ adopts a tetragonal Ruddlesden–Popper structure [space group $I4/mmm$, $a = 3.87458(6)$, $c = 19.9962(3)$ Å, $R_{\text{wpr}} = 9.24\%$].

Magnetic susceptibility and resistivity data for $\text{LaSr}_2\text{Mn}_2\text{O}_7$ are shown in Figs. 2 and 3 respectively. The sharp increase in magnetisation at 132 K may be assigned to a transition to a weak ferromagnetic state (the low-temperature magnetisation corresponds to a moment of $0.35 \mu_B$ per Mn) and magnetisation measurements below this temperature clearly show hysteresis. The key point is that the resistivity measurements show a

change in sign of $d\rho/dT$ at the temperature where the magnetisation increases sharply, indicating that the onset of weak ferromagnetism in the Ruddlesden–Popper phase is strongly correlated with the charge transport and drives a metal–insulator transition. Grain boundary effects will mean that the measured resistivity is an upper limit, and the coincidence of the transition temperature in the electrical and magnetic measurements leads us to conclude that we are observing a bulk effect. The partially parallel spin alignment at neighbouring sites facilitates near-neighbour electron hops by lowering the on-site repulsion energy barrier. The activation energy is $0.109(1)$ eV

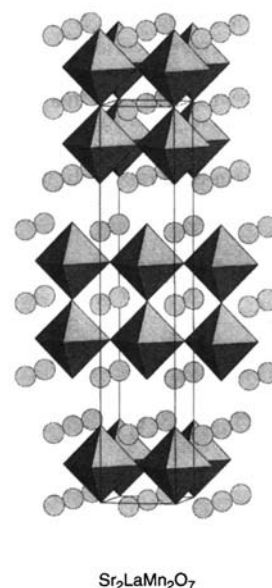


Fig. 1 The Ruddlesden–Popper crystal structure of $\text{LaSr}_2\text{Mn}_2\text{O}_7$. MnO_6 octahedra are shaded and the A sites (occupied in a disordered manner by the lanthanide and alkaline-earth cations) are shown as spheres.

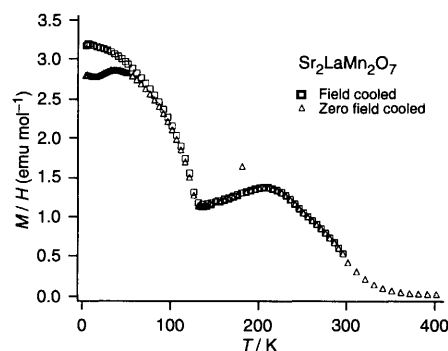


Fig. 2 The field-cooled and zero-field-cooled magnetisation of $\text{LaSr}_2\text{Mn}_2\text{O}_7$ measured in a field of 0.1 T as a function of temperature (data are displayed as the measured magnetisation divided by the applied field—this is strictly equal to the susceptibility above 370 K)

in the semiconducting phase over the range $211 < T/K < 300$.

The new phase $\text{Sr}_2\text{TbMn}_2\text{O}_7$ provides an important contrast with $\text{Sr}_2\text{LaMn}_2\text{O}_7$ —although X-ray Rietveld refinement indicates the two materials are isostructural [for $\text{TbSr}_2\text{Mn}_2\text{O}_7$ $a = 3.8204(1)$, $c = 19.9833(8)$ Å], the magnetic susceptibility of the Tb system (Fig. 4) obeys the Curie–Weiss law with a magnetic moment of $12.73 \mu_B$ per formula unit between 50 and 300 K (this compares with a theoretical value of $11.55 \mu_B$ calculated on the basis of the oxidation state distribution $\text{Sr}_2\text{Tb}^{\text{III}}\text{Mn}^{\text{III}}\text{Mn}^{\text{IV}}\text{O}_7$). Samples prepared in air and oxygen show identical magnetic behaviour. Although there is apparently a magnetic anomaly at *ca.* 40 K and a small amount of hysteresis is found in magnetisation measurements at 5 K, there is no metal–insulator transition driven by weak ferromagnetism and the compound is a semiconductor, albeit with a variable activation energy (*ca.* 0.14 eV) between 4.2 and 300 K. No hysteresis is apparent in the resistivity of the Tb compound, in contrast to that of the La analogue.

Interestingly, the room-temperature molar magnetisation of $\text{Sr}_2\text{TbMn}_2\text{O}_7$ is considerably less than that of the La material, and in contrast to $\text{Sr}_2\text{LaMn}_2\text{O}_7$, the magnetisation is well fitted by a Curie–Weiss law over a wide temperature range. The magnetic behaviour of $\text{Sr}_2\text{LaMn}_2\text{O}_7$ is complex over the region studied, with linear magnetisation curves but remanent zero-field magnetisation even at room temp., suggesting that superparamagnetic domains may be the cause of the enhance susceptibility. The drop in the magnetisation at 370 K occurs together with a loss of remanence in the zero-field magnetisation, although the new truly paramagnetic magnetisation is still consistent with a larger moment than that calculated from non-interacting manganese ions alone (9.8 vs. $4.4 \mu_B$). Preliminary neutron powder diffraction measurements have shown that magnetic order is present on a relatively large distance scale at 150 K, *i.e.* above the metal–insulator transition. The observation

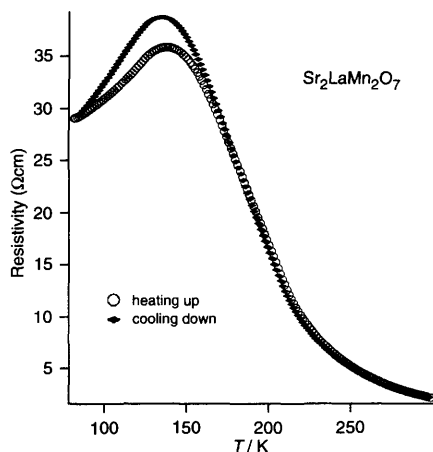


Fig. 3 Electrical resistivity of $\text{LaSr}_2\text{Mn}_2\text{O}_7$ as a function of temperature

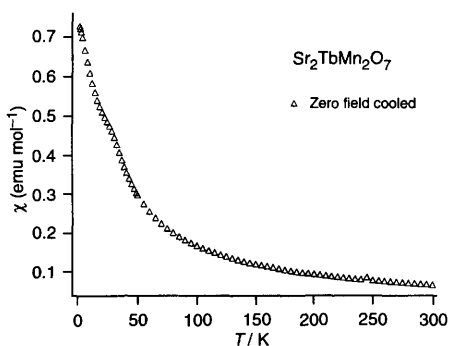


Fig. 4 Magnetic susceptibility of $\text{TbSr}_2\text{Mn}_2\text{O}_7$ measured in a field of 0.1 T as a function of temperature

of purely magnetic Bragg peaks shows that the ordering has an antiferromagnetic component to it. It seems possible that the transition at 132 K involves the alignment and merger of weakly ferromagnetic domains, the size of which increases between 370 and 132 K. The reduction in the domain wall density eliminates an electron scattering mechanism and a metal–insulator transition results.

To conclude, we have observed a metal–insulator transition driven by the onset of weak ferromagnetism in the $n = 2$ Ruddlesden–Popper phase $\text{LaSr}_2\text{Mn}_2\text{O}_7$. There are important differences in the electronic properties of the $n = 2$ series from the more familiar $n = 1$ and $n = \infty$ two- and three-dimensional limiting phases, which are semiconducting at an Mn oxidation state of +3.5 due to localisation of the carriers on distinct Mn^{III} and Mn^{IV} sites ('charge ordering').^{4,8} Characterisation of the new Tb phase shows that the weak ferromagnetism, the associated metal–insulator transition and the unusually large magnetisation observed for $\text{Sr}_2\text{LaMn}_2\text{O}_7$ are suppressed with the smaller, more readily oxidised terbium as the lanthanide counter cation. This cation dependence is more marked in the Ruddlesden–Popper phases than in the perovskite systems,⁹ thus suggesting that there is more scope for chemical control of the electronic properties in the former. The fact that the unit-cell contraction which occurs when La is replaced by Tb is markedly anisotropic may be important in explaining the changes occurring in the electronic properties.

We are grateful to EPSRC and the Donors of The Petroleum Research Fund, administered by the American Chemical Society, for financial support. We thank Dr J. P. Attfield for allowing us access to the SQUID magnetometer at the IRC in Superconductivity at the University of Cambridge.

Footnote

† $\text{LaSr}_2\text{Mn}_2\text{O}_7$ was prepared by firing dry La_2O_3 , MnO_2 and SrCO_3 in alumina boats in air at 800 °C for 12 h, 1000 °C for 24 h and 1200 °C for 24 h, then regrinding, pelletising and firing for 4 days at 1400 °C with one further regrind. $\text{Sr}_2\text{TbMn}_2\text{O}_7$ was prepared in a similar manner and is stable in both air and oxygen atmospheres. Compositions were confirmed by ICP atomic emission analysis: observed and calculated percentages are (i) $\text{LaSr}_2\text{Mn}_2\text{O}_7$ La 25.6/25.9, Sr 32.8/32.7, Mn 21.5/20.5; (ii) $\text{TbSr}_2\text{Mn}_2\text{O}_7$ Tb 29.0/28.6, Sr 32.0/31.5, Mn 20.3/19.8. Magnetic measurements were performed on a Quantum Design MPMS magnetometer between 0 and 5 T and 4.2 and 400 K. Electrical conductivity measurements were carried out using the 4 probe dc technique between 4.2 and 300 K (Tb) or 80 and 300 K (La). Silver contacts were painted onto sintered polycrystalline bars. Powder X-ray data were collected in Bragg–Brentano geometry on a Siemens D5000 diffractometer (Cu-K α_1 radiation) and Rietveld analysis was performed using the GSAS suite of programs. All resulting bond lengths and angles were chemically reasonable, with the shortest oxide–oxide contact being 2.74(1) Å. Neutron diffraction data were collected on the powder diffractometer D1B at ILL Grenoble.

References

- 1 R. M. Kusters, J. Singleton, D. A. Keen, R. McGreevy and W. Hayes, *Physica B*, 1989, **155**, 362.
- 2 R. von Helmholt, J. Wecker, B. Holzapfel, L. Schultz and K. Samwer, *Phys. Rev. Lett.*, 1993, **71**, 2331.
- 3 S. Jin, T. H. Tiefel, M. McCormack, R. A. Fastnacht, R. Ramesh and L. H. Chen, *Science*, 1994, **264**, 413.
- 4 Y. Moritomo, Y. Tomioka, A. Asamitsu, Y. Tokura and Y. Matsui, *Phys. Rev. B*, 1995, **51**, 3297.
- 5 J. B. MacChesney, J. F. Potter and R. C. Sherwood, *J. Appl. Phys.*, 1969, **40**, 1243.
- 6 R. A. Mohan Ram, P. Ganguly and C. N. R. Rao, *J. Solid State Chem.*, 1987, **70**, 82.
- 7 K. Knizek, Z. Jirak, E. Pollert, F. Zounova and S. Vratilav, *J. Solid State Chem.*, 1992, **100**, 292.
- 8 Y. Tomioka, A. Asamitsu, Y. Moritomo, H. Kuwahara and Y. Tokura, *Phys. Rev. Lett.*, 1995, **74**, 5108.
- 9 V. Caignaert, A. Maignan and B. Raveau, *Solid State Commun.*, 1995, **95**, 357.

Received, 4th December 1995; Com. 5107846F